Error analysis of mixed finite element methods for nonlinear parabolic equations

Huadong Gao [*]   and   Weifeng Qiu [†]

July 11, 2017

Abstract

In this paper, we prove a discrete embedding inequality for the Raviart–Thomas mixed finite element methods for second order elliptic equations, which is analogous to the Sobolev embedding inequality in the continuous setting. Then, by using the proved discrete embedding inequality, we provide an optimal error estimate for linearized mixed finite element methods for nonlinear parabolic equations. Several numerical examples are provided to confirm the theoretical analysis.

Keywords: nonlinear parabolic equations, finite element method, discrete Sobolev embedding inequality, unconditional convergence, optimal error analysis

AMS subject classifications. 35Q30, 65M60, 65N30.

1   Introduction

Since the pioneering work of Raviart and Thomas [27], mixed finite element methods (FEMs) have proved to be a fundamental tool to numerically solve various problems arising in physics and engineering sciences. Mixed FEMs have many attractive features over the conventional Lagrange FEMs. For instance, mixed FEMs conserve mass locally, which is of crucial importance in numerical methods for flow coupled to transport, see [10]. By introducing ∇u as an extra variable, mixed methods can produce accurate flux approximations. Mixed FEMs are also more robust in the case of low regularity of nonsmooth coefficients. We refer to the monographs [3, 12] for the general theory of Mixed FEMs. There are numerous applications of Raviart–Thomas mixed FEMs, etc., see [6, 16, 17, 22, 23, 28] for general linear and nonlinear parabolic equations, [4, 14, 19] for semiconductor modeling, [1, 2] for porous media flow problems.

In this paper, we consider the mixed finite element methods(FEMs) for nonlinear parabolic equations

$$
\begin{cases}
\dfrac{\partial u}{\partial t} - \Delta u + f(u, \nabla u) = 0, & \text{in } \Omega \times (0, T], & (1.1) \\[2mm]
u(\boldsymbol{x}, t) = u^0(\boldsymbol{x}), & \text{in } \Omega, & (1.2) \\[2mm]
u = 0, & \text{on } \partial\Omega, & (1.3)
\end{cases}
$$

where f is a given function. We assume Ω is a bounded Lipschitz polygonal/polyhedral domain in $\mathbb{R}^d (d = 2, 3)$. There have been extensive works on mixed methods for the above equations (1.1)-(1.3). We give a brief summary along with some representative (but certainly not exhaustive) requirement for the function $f(u, \nabla u)$ (or $f(u)$) in the literature.

- The function $f(u)$ is a smooth function of $u \in \mathbf{R}$, i.e., there exists a bound B_1 such that

$$|f^{(i)}| \leq B_1, \quad i = 0, 1, 2, \dots$$

see page 270 of [23].
- There exists a bound k_1 such that, for every $u \in \mathbf{R}$

$$|f| \leq k_1, \quad \left|\frac{\partial f}{\partial u}\right| \leq k_1$$

See page 131 of [16] and page 150 of [17].
- The function $f(\boldsymbol{x}, , u) : \overline{\Omega} \times \mathbf{R} \to \mathbf{R}$ is a triple continuously differential function with bounded derivatives up to the third order. See page 205 of [6], page 410 of [7] and page 195 of [8].
- The reaction term f is twice continuously differential on Ω with bounded derivatives up to the second order. See page 322 of [28].

Let us examine why all the above works need these strong assumptions on f. It is not difficult to deduce that, under the above requirements on f, the error between $f(u)$ and $f(u_h)$ can be bounded by

$$\|f(u) - f(u_h)\|_{L^2} \leq \|f'(\xi_{u_h, u})(u - u_h)\|_{L^2} \leq \max_{x \in \mathbf{R}} |f'(x)| \|(u - u_h)\|_{L^2} \leq C\|u - u_h\|_{L^2}.$$

where C is a constant independent of u, u_h and the mesh size h. Due to these severe restrictions on f in [16, 17, 6, 7, 8, 23, 28], the "nonlinear" problem (1.1)-(1.3) can be almost reduced to a linear one. Clearly, these assumptions on f cannot be satisfied in most applications. For instance, $f(u) = u^3 - u$ is frequently used in phase field problems and nonlinear Schrodinger equations; $f(u) = (\mathbf{b} \cdot \nabla u)u$ where $\mathbf{b} = [1, 1, 1]^T$ appears in the viscous Burgers' equation. In these two cases, f does not satisfies the conditions in [6, 7, 8, 16, 17, 23, 28]. Thus, all previous results are not applicable. To eliminate the strong assumptions of f and also control the nonlinear term $f(u, \nabla u)$, one must derive a uniform boundedness of u_h in certain strong norms. If conventional Lagrange elements are used, one popular linearized FEM for the equation (1.1) is to seek $u_h^n \in P_h^r \subset H^1(\Omega)$ such that

$$\left(\frac{u_h^n - u_h^{n-1}}{\tau}, v_h\right) + (\nabla u_h^n, \nabla v_h) + (f(u_h^{n-1}, \nabla u_h^n), v_h) = 0, \qquad \forall v_h \in P_h^r \subset H^1(\Omega). \qquad (1.4)$$

And it is easy to see that $u_h \in H^1(\Omega)$ satisfies

$$\begin{cases} \|u_h\|_{L^p} \leq C\|\nabla u_h\|_{L^2}, & \text{for } 1 \leq p < +\infty, \quad \text{in two-dimensional space} \\ \|u_h\|_{L^p} \leq C\|\nabla u_h\|_{L^2}, & \text{for } 1 \leq p \leq 6, \quad \text{in three-dimensional space}, \end{cases}$$

where $\|\nabla u_h\|_{L^2}$ naturally arise in the discretization of the diffusion terms. By using this technique, unconditionally optimal error estimates of conventional Lagrange FEMs were established in [15, 20] for several nonlinear parabolic problems. On the contrary, if mixed FEMs are used for spatial discretizations, a linearized mixed FEM is to seek $(\boldsymbol{\sigma}_h^n, u_h^n) \in \mathbf{H}_h^r \times V_h^r \subset \mathbf{H}(\text{div}) \times L^2$, such that

$$\begin{cases} (\boldsymbol{\sigma}_h^n, \boldsymbol{\chi}_h) + (u_h^n, \text{div}\boldsymbol{\chi}_h) = 0, & \forall \boldsymbol{\chi}_h \in \mathbf{H}_h^r, \qquad (1.5) \\ \left(\frac{u_h^n - u_h^{n-1}}{\tau}, v_h\right) - (\text{div}\boldsymbol{\sigma}_h^n, v_h) + (f(u_h^{n-1}, \boldsymbol{\sigma}_h^{n-1}), v_h) = 0, & \forall v_h \in V_h^r, \qquad (1.6) \end{cases}$$

2

where $\mathbf{H}_h^r \times V_h^r$ are the Raviart–Thomas mixed finite element spaces, see the definition in section 2. It is easy to see that for the mixed scheme (1.5)-(1.6) one can only derive

$$\frac{\|u_h^n\|^2 - \|u_h^n\|^2}{2\tau} + \frac{1}{2\tau}\|u_h^n - u_h^{n-1}\| + \|\boldsymbol{\sigma}_h\|_{L^2}^2 + (f(u_h^{n-1}, \boldsymbol{\sigma}_h^{n-1}), u_h) = 0.$$

Therefore, we must use $\|\boldsymbol{\sigma}_h\|_{L^2}^2$ to control the nonlinear term $f(u_h^{n-1}, \boldsymbol{\sigma}_h^{n-1})$. More precisely, we shall establish embedding inequalities between u_h^n and $\boldsymbol{\sigma}_h^n$

$$\begin{cases} \|u_h^n\|_{L^p} \le C\|\boldsymbol{\sigma}_h^n\|_{L^2}, & \text{for } 1 \le p < \infty, \quad \text{in two-dimensional space,} \\ \|u_h^n\|_{L^p} \le C\|\boldsymbol{\sigma}_h^n\|_{L^2}, & \text{for } 1 \le p \le 6, \quad \text{in three-dimensional space,} \end{cases}$$

Although the above results seems rather reasonable, to the best our knowledge, such a relationship for $(\boldsymbol{\sigma}_h, u_h)$ is unavailable in the literature. In this paper, we provide a rigorous proof for the discrete Sobolev embedding inequalities for the Raviart–Thomas mixed FEMs. A key step in our proof is to introduce a new norm $\|u_h\|_{DG}$, which can be viewed as the broken H^1 norm of u_h. Then, we analyze $\|u_h\|_{DG}$ and $\|\boldsymbol{\sigma}_h\|$ carefully to derive the desired results.

The rest of this paper is organized as follows. In section 2, we provide some notations and lemmas for later use. In section 3, we prove the discrete Sobolev embedding inequalities associated to the Raviart–Thomas mixed FEMs. In section 4, we provide an optimal error estimate for the linearized mixed FEMs by using the discrete Sobolev embedding inequalities. Numerical examples in both two- and three-dimensional spaces are given in section 5 to confirm the error estimates and show the efficiency of linearized mixed FEMs.

2 Preliminaries

Let $W^{k,p}(\Omega)$ be the Sobolev space defined on Ω, and by conventional notations, $H^k(\Omega) := W^{k,2}(\Omega)$. To introduce the mixed formulation, we denote

$$\mathbf{H}(\mathrm{div}; \Omega) = \left\{ \boldsymbol{u} \,\middle|\, \boldsymbol{u} \in \mathbf{L}^2(\Omega), \mathrm{div}\, \boldsymbol{u} \in L^2(\Omega) \right\} \text{ with } \|\boldsymbol{u}\|_{\mathbf{H}(\mathrm{div})} = \left(\|\boldsymbol{u}\|_{L^2}^2 + \|\mathrm{div}\, \boldsymbol{u}\|_{L^2}^2 \right)^{\frac{1}{2}}$$

and its dual space $\mathring{\mathbf{H}}(\mathrm{div})'$ with norm

$$\|\boldsymbol{v}\|_{\mathring{\mathbf{H}}(\mathrm{div})'} := \sup_{\boldsymbol{w} \in \mathring{\mathbf{H}}(\mathrm{div})} \frac{(\boldsymbol{v}, \boldsymbol{w})}{\|\boldsymbol{w}\|_{\mathbf{H}(\mathrm{div})}}.$$

Let $\mathcal{T}_h = \{K\}$ be a regular mesh partition of Ω and denote the mesh size $h = \max_K\{\mathrm{diam}K\}$. By $\mathcal{F}_h$ we denote all the $(d-1)$-dimensional faces of the partition $\mathcal{T}_h$. We define the Raviart–Thomas finite element spaces by

$$\begin{cases} \mathbf{H}_h^r(\Omega) := \{\boldsymbol{q} \in \mathbf{H}(\mathrm{div}; \Omega) \quad : \quad \boldsymbol{q}|_K \in [P_r(K)]^d + \boldsymbol{x}P_r(K), \quad \forall K \in \mathcal{T}_h\}, \\ V_h^r(\Omega) := \{u \in L^2(\Omega) \quad : \quad u|_K \in P_r(K), \quad \forall K \in \mathcal{T}_h\}, \end{cases}$$

where $P_r(K)$ is the space of polynomials of degree r or less defined on K. It is well-known that $\mathbf{H}_h^r(\Omega) \times V_h^r(\Omega)$ is a stable finite element pair for solving the second order elliptic problems, see [3, 22, 25, 27]. Let $\{t_n\}_{n=0}^N$ be a uniform partition in the time direction with the step size $\tau = \frac{T}{N}$. For a sequence of functions $\{u^n\}$ defined on Ω, we denote the backward Euler discretization operator

$$D_\tau u^n = \frac{u^n - u^{n-1}}{\tau}.$$

3

In the rest part of this paper, for simplicity of notation we denote by C a generic positive constant and ϵ a generic small positive constant, which are independent of n, h and τ. We present the Gagliardo–Nirenberg and discrete Gronwall's inequalities in the following lemmas which will be frequently used in our proofs.

Lemma 2.1. (Gagliardo–Nirenberg inequality [26]): Let u be a function defined on Ω in $\mathbb{R}^d$ and $\partial^s u$ be any partial derivative of u of order s, then

$$\|\partial^j u\|_{L^p} \leq C\|\partial^m u\|_{L^r}^a \|u\|_{L^q}^{1-a} + C\|u\|_{L^q},$$

for $0 \leq j < m$ and $\frac{j}{m} \leq a \leq 1$ with

$$\frac{1}{p} = \frac{j}{d} + a\left(\frac{1}{r} - \frac{m}{d}\right) + (1-a)\frac{1}{q},$$

except $1 < r < \infty$ and $m - j - \frac{n}{r}$ is a non-negative integer, in which case the above estimate holds only for $\frac{j}{m} \leq a < 1$.

Lemma 2.2. Discrete Gronwall's inequality [18] : Let τ, B and a_k, b_k, c_k, γ_k, for integers $k \geq 0$, be non-negative numbers such that

$$a_n + \tau \sum_{k=0}^{n} b_k \leq \tau \sum_{k=0}^{n} \gamma_k a_k + \tau \sum_{k=0}^{n} c_k + B, \quad \text{for} \quad n \geq 0,$$

suppose that $\tau\gamma_k < 1$, for all k, and set $\sigma_k = (1 - \tau\gamma_k)^{-1}$. Then

$$a_n + \tau \sum_{k=0}^{n} b_k \leq \exp(\tau \sum_{k=0}^{n} \gamma_k \sigma_k)(\tau \sum_{k=0}^{n} c_k + B), \quad \text{for} \quad n \geq 0.$$

3 Discrete Sobolev embedding inequalities of mixed FEMs for the Poisson problem

We consider in this section the model problem

$$\begin{cases} -\Delta u = f, & \text{for } x \in \Omega, \\ u = 0, & \text{for } x \in \partial\Omega. \end{cases}$$

The standard Raviart–Thomas mixed FEM for the above model problem is to seek $(\boldsymbol{\sigma}_h, u_h) \in \mathbf{H}_h^r(\Omega) \times V_h^r(\Omega)$ such that

$$\begin{cases} (\boldsymbol{\sigma}_h, \boldsymbol{\chi}_h) + (u_h, \operatorname{div}\boldsymbol{\chi}_h) = 0, & \forall \boldsymbol{\chi}_h \in \mathbf{H}_h^r(\Omega), & (3.1) \\ (\operatorname{div}\boldsymbol{\sigma}_h, v_h) = -(f, v_h), & \forall v_h \in V_h^r(\Omega). & (3.2) \end{cases}$$

Error analyses for the above mixed methods (3.1)-(3.2) can be found in [3, 25, 27] and references therein. The mixed methods computes the original unknown u_h and the flux $\boldsymbol{\sigma}_h$ simultaneously. On the contrary, to obtain the flux ∇u, conventional Lagrange FEMs need to use certain numerical differentiation, which may lead to a loss in accuracy. If we still denote by u_h the conventional Lagrange FEM solution to the above Poisson problem, then u_h satisfies the following Sobolev inequalities

$$\begin{cases} \|u_h\|_{L^p} \leq C\|\nabla u_h\|_{L^2}, & \text{for } 1 \leq p < \infty, \quad \text{in two-dimensional space,} & (3.3) \\ \|u_h\|_{L^p} \leq C\|\nabla u_h\|_{L^2}, & \text{for } 1 \leq p \leq 6, \quad \text{in three-dimensional space,} & (3.4) \end{cases}$$

4

which inherits the H^1 conforming nature. As $\boldsymbol{\sigma}_h$ numerically converges to ∇u, one may ask whether similar Sobolev embedding inequalities hold for the mixed FEM solutions $(\boldsymbol{\sigma}_h, u_h)$. In this section, we give an affirmative answer to this question and provide a proof.

The main idea used in the proof is to investigate the relationship between mixed FEMs and the discontinuous Galerkin FEMs. The reasons are twofold: Firstly, there have been powerful tools developed for the discontinuous Garkerkin methods, see [5, 9]; Secondly, the numerical solution u_h is in the discontinuous finite element space but not in $H^1(\Omega)$. Following [9], we define the $\| \cdot \|_{DG}$ norm of u_h by

$$\|u_h\|_{DG}^2 := \sum_{K \in \mathcal{T}_h} \int_K |\nabla u_h|^2 \mathrm{d}x + \sum_{F \in \mathcal{F}_h} \frac{1}{h_F} \int_F |[\![u_h]\!]|^2 \mathrm{d}x, \tag{3.5}$$

where h_F denotes the size of the face F. For two adjacent elements K and K' sharing the same face F, the jump of a function $u_h \in V_h^r(\Omega)$ across F is defined by

$$[\![u_h]\!] = u_h|_{\partial K \cap F} - u_h|_{\partial K' \cap F}.$$

In case of $F \in \partial K$ lying on $\partial\Omega$, we define $[\![u_h]\!] := u_h|_{\partial K \cap F}$. The main results obtained in [9] are the following discrete Sobolev embedding inequalities

$$\begin{cases} \|u_h\|_{L^p} \le C\|u_h\|_{DG}, & \text{for } 1 \le p < \infty, \quad \text{in two-dimensional space}, \tag{3.6} \\ \|u_h\|_{L^p} \le C\|u_h\|_{DG}, & \text{for } 1 \le p \le 6, \quad \text{in three-dimensional space}, \tag{3.7} \end{cases}$$

where C is a constant depending upon the domain Ω, r and p only. We will show in Theorem 3.2 that $\|u_h\|_{DG}$ is bounded by $\|\boldsymbol{\sigma}_h\|_{L^2}$. Before going further, we consider the following projection problem for the Raviart–Thomas element, which will be used in the later proof. This lemma first appears in [11]. Here we provide a complete proof with details.

Lemma 3.1. *For each element $K \in \mathcal{T}_h$, given $\boldsymbol{p} \in [L^2(K)]^d$, $q_i \in L^2(F_i)$ where $\{F_i\} \in \partial K$, there exists a unique $\boldsymbol{\zeta}_h \in RT_r(K)$ such that*

$$\begin{cases} \displaystyle\int_K (\boldsymbol{\zeta}_h - \boldsymbol{p}) \cdot \boldsymbol{\omega}_h \, dx = 0, & \forall \boldsymbol{\omega}_h \in [P_{r-1}(K)]^d, \tag{3.8} \\ \displaystyle\int_{F_i} (\boldsymbol{\zeta}_h \cdot \mathbf{n}_{F_i} - q_i) \, \mu_h \, dx = 0, & \forall \mu_h \in P_r(F_i), \tag{3.9} \end{cases}$$

where $RT_r(K)$ is the restriction of the Raviart–Thomas element space $\mathbf{H}_h^r(\Omega)$ on K. More importantly, the following stability holds

$$\|\boldsymbol{\zeta}_h\|_{L^2(K)}^2 \le C \left(\|\boldsymbol{p}\|_{L^2(K)}^2 + \sum_{F_i \in \partial K} h\|q_i\|_{L^2(F_i)}^2 \right), \tag{3.10}$$

where C is independent of h and K.

Proof: The equation numbers in (3.8)-(3.9) satisfy

$$\underbrace{d\binom{d+r-1}{r-1}}_{\text{eqn. (3.8)}} + \underbrace{(d+1)\binom{d+r-1}{r}}_{\text{eqn. (3.9)}} = \underbrace{\frac{(d+r+1)\,(d+r-1)!}{(d-1)!r!}}_{\dim\{RT_r(K)\}},$$

which immediately yields the the existence and uniqueness of the projection. We prove (3.10) by a scaling argument. To do so, let $\widehat{K}$ be the reference element, which can be a simplex in $\mathbb{R}^d$.

5

Given $\widehat{\boldsymbol{p}} \in [L^2(\widehat{K})]^d$, $\widehat{q}_i \in L^2(\widehat{F}_i)$ where $\{\widehat{F}_i\} \in \partial\widehat{K}$, the corresponding projection on $\widehat{K}$ is to seek $\widehat{\boldsymbol{\zeta}}_h \in RT_r(\widehat{K})$ such that

$$\begin{cases} \displaystyle\int_{\widehat{K}} (\widehat{\boldsymbol{\zeta}}_h - \widehat{\boldsymbol{p}}) \cdot \widehat{\boldsymbol{\omega}}_h \mathrm{d}\hat{x} = 0\,, & \forall \widehat{\boldsymbol{\omega}}_h \in [P_{r-1}(\widehat{K})]^d\,, & (3.11) \\[2mm] \displaystyle\int_{\widehat{F}_i} (\widehat{\boldsymbol{\zeta}}_h \cdot \mathbf{n}_{\widehat{F}_i} - \widehat{q}_i)\,\widehat{\mu}_h \mathrm{d}\hat{x} = 0\,, & \forall \widehat{\mu}_h \in P_r(\widehat{F}_i)\,. & (3.12) \end{cases}$$

The existence and uniqueness of $\widehat{\boldsymbol{\zeta}}_h$ are obvious. Furthermore, it is easy to derive that

$$\left\| \widehat{\boldsymbol{\zeta}}_h \right\|_{L^2(\widehat{K})}^2 \le C \Big(\|\widehat{\boldsymbol{p}}\|_{L^2(\widehat{K})}^2 + \sum_{\widehat{F}_i \in \partial\widehat{K}} \|\widehat{q}_i\|_{L^2(\widehat{F}_i)}^2 \Big) \tag{3.13}$$

where C depends upon $\widehat{K}$ and r only. To build a connection between $\widehat{K}$ and K, we define the affine mapping $T_K : \mathbb{R}^d \to \mathbb{R}^d$ by

$$T_K := B_K \widehat{x} + b_k, \quad \forall \widehat{x} \in \mathbb{R}^d. \tag{3.14}$$

We also note that for $\{\widehat{F}_i\} \in \partial\widehat{K}$, $T_K(\widehat{F}_i) = F_i$. Then, for a scalar function $\phi \in H^1(K)$, we define

$$\widehat{\phi} = \phi \circ T_K \tag{3.15}$$

For $\boldsymbol{\zeta} \in [H^1(K)]^d$, we shall introduce the Piola transformation

$$\widehat{\boldsymbol{\zeta}} = |\det B_K|\, B_K^{-1}\, \boldsymbol{\zeta} \circ T_K. \tag{3.16}$$

With the above transformations (3.14)-(3.16), the projection (3.8)-(3.9) can be rewritten by

$$\begin{cases} \displaystyle\int_{\widehat{K}} \left(\widehat{\boldsymbol{\zeta}}_h - \widehat{\boldsymbol{p}} \right) \cdot \widehat{\boldsymbol{\omega}}_h \mathrm{d}\hat{x} = 0\,, & \forall \widehat{\boldsymbol{\omega}}_h \in [P_{r-1}(\widehat{K})]^d\,, & (3.17) \\[2mm] \displaystyle\int_{\widehat{F}_i} \left(\widehat{\boldsymbol{\zeta}}_h \cdot \mathbf{n}_{\widehat{F}_i} - \frac{|F_i|}{|\widehat{F}_i|} \widehat{q}_i \right) \widehat{\mu}_h \mathrm{d}\hat{x} = 0\,, & \forall \widehat{\mu}_h \in P_r(\widehat{F}_i)\,. & (3.18) \end{cases}$$

where the Piola transformation (3.16) is used for the vector functions $\boldsymbol{\zeta}_h$, $\boldsymbol{p}$ and $\boldsymbol{\omega}_h$, and affine transformation (3.15) is used for $\{q_i\}$ and μ_h, respectively. Finally, we use the scaling argument to derive that

$$\begin{aligned} \|\boldsymbol{\zeta}_h\|_{L^2(K)} &\le \|B_K\|\, |\det B_K|^{-\frac{1}{2}} \|\widehat{\boldsymbol{\zeta}}_h\|_{L^2(\widehat{K})} \\[2mm] &\le C\|B_K\|\, |\det B_K|^{-\frac{1}{2}} \left(\|\widehat{\boldsymbol{p}}\|_{L^2(\widehat{K})} + \sum_{\widehat{F}_i \in \partial\widehat{K}} \frac{|F_i|}{|\widehat{F}_i|} \|\widehat{q}_i\|_{L^2(\widehat{F}_i)} \right) \\[2mm] &\le C\|B_K\|\, |\det B_K|^{-\frac{1}{2}} \left(|\det B_K|^{\frac{1}{2}} \|B_K^{-1}\| \|\boldsymbol{p}\|_{L^2(K)} + \sum_{F_i \in \partial K} \left(\frac{|F_i|}{|\widehat{F}_i|} \right)^{1/2} \|q_i\|_{L^2(F_i)} \right) \\[2mm] &\le C\|B_K\| \|B_K^{-1}\| \|\boldsymbol{p}\|_{L^2(K)} + C \sum_{F_i \in \partial K} \|B_K\|\, |\det B_K|^{-\frac{1}{2}} \left(\frac{|F_i|}{|\widehat{F}_i|} \right)^{1/2} \|q_i\|_{L^2(F_i)} \\[2mm] &\le C \left(\|\boldsymbol{p}\|_{L^2(K)} + h^{\frac{1}{2}} \sum_{F_i \in \partial K} \|q_i\|_{L^2(F_i)} \right), \end{aligned}$$

where we have used estimate (3.13) and noted the fact that $\mathcal{T}_h$ is shape regular(h and h_F are equivalent). By squaring the above inequality, we get the desired estimate (3.10) directly. $\square$

Now, we are ready to prove the discrete Sobolev embedding inequalities for the mixed FEM solutions $(\boldsymbol{\sigma}_h, u_h)$, which play a key role in the unconditionally optimal error analysis in the next section 4.

Theorem 3.2. *For any given $u_h \in V_h^r(\Omega)$, if there exists a $\boldsymbol{\sigma}_h \in \mathbf{H}_h^r(\Omega)$ such that*

$$(\boldsymbol{\sigma}_h, \boldsymbol{\chi}_h) + (u_h, \mathrm{div}\boldsymbol{\chi}_h) = 0, \qquad \forall \boldsymbol{\chi}_h \in \mathbf{H}_h^r(\Omega), \tag{3.19}$$

then the following discrete Sobolev embedding inequality holds

$$\begin{cases} \|u_h\|_{L^p} \le C\|\boldsymbol{\sigma}_h\|_{L^2}, & \text{for } 1 \le p < \infty, & \text{in two dimensional space}, & (3.20) \\ \|u_h\|_{L^p} \le C\|\boldsymbol{\sigma}_h\|_{L^2}, & \text{for } 1 \le p \le 6, & \text{in three dimensional space}, & (3.21) \end{cases}$$

where C is a constant only depending upon the domain, r and p.

Proof: By using integration by parts for the equation (3.19), we have

$$\begin{aligned} 0 &= (\boldsymbol{\sigma}^n, \boldsymbol{\chi}_h) + (u_h, \mathrm{div}\boldsymbol{\chi}_h) \\ &= (\boldsymbol{\sigma}^n, \boldsymbol{\chi}_h) + \sum_{K \in \mathcal{T}_h} \int_K u_h \mathrm{div}\boldsymbol{\chi}_h \mathrm{d}x \\ &= (\boldsymbol{\sigma}^n, \boldsymbol{\chi}_h) + \sum_{K \in \mathcal{T}_h} \left(- \int_K \nabla u_h \cdot \boldsymbol{\chi}_h \mathrm{d}x + \int_{\partial K} u_h \, \boldsymbol{\chi}_h \cdot \mathbf{n}_K \, \mathrm{d}s \right) \\ &= (\boldsymbol{\sigma}^n, \boldsymbol{\chi}_h) - \sum_{K \in \mathcal{T}_h} \int_K \nabla u_h \cdot \boldsymbol{\chi}_h \mathrm{d}x + \sum_{F \in \mathcal{F}_h} \int_F [\![u_h]\!] \boldsymbol{\chi}_h \cdot \mathbf{n}_F \mathrm{d}x. \end{aligned} \tag{3.22}$$

Then, on each element K, we require $\boldsymbol{\chi}_h$ to be the projection, such that

$$\begin{cases} \displaystyle\int_K (\boldsymbol{\chi}_h - \nabla u_h) \cdot \boldsymbol{\omega}_h \mathrm{d}x = 0, & \forall \boldsymbol{\omega}_h \in [P_{r-1}(K)]^d, \\ \displaystyle\int_{F_i} \left(\boldsymbol{\chi}_h \cdot \mathbf{n}_{F_i} + \frac{1}{h_{F_i}} [\![u_h]\!]\right) \mu_h \mathrm{d}x = 0, & \forall \mu_h \in P_r(F_i). \end{cases}$$

Lemma 3.1 tells that such a $\boldsymbol{\chi}_h \in \mathbf{H}_h^r(\Omega)$ exists and is unique, which also satisfies

$$\|\boldsymbol{\chi}_h\|_{L^2(K)}^2 \le C \left(\|\nabla u_h\|_{L^2(K)}^2 + \sum_{F_i \in \partial K} \frac{1}{h} \|[\![u_h]\!]\|_{L^2(F_i)}^2 \right)$$

Substituting this $\boldsymbol{\chi}_h$ into (3.22) yields

$$\|u_h\|_{DG}^2 \le (\boldsymbol{\sigma}_h, \boldsymbol{\chi}_h) \le \|\boldsymbol{\sigma}_h\|_{L^2(\Omega)} \|\boldsymbol{\chi}_h\|_{L^2(\Omega)} \le C\|\boldsymbol{\sigma}_h\|_{L^2(\Omega)} \|u_h\|_{DG}.$$

The discrete Sobolev embedding inequalities (3.20)-(3.21) follows directly from (3.6)-(3.7) and the last inequality. The theorem is proved. $\square$

Remark 3.3. *In the above proof, we can see that $\boldsymbol{\sigma}_h$ can be replaced by any $\boldsymbol{f} \in \mathbf{L}^2(\Omega)$.*

4 Applications in unconditionally optimal error estimates of nonlinear parabolic equations

4.1 Linearized mixed FEMs for nonlinear parabolic equations

In this section, we employ the discrete Sobolev embedding inequalities to establish an unconditionally optimal error estimates of linearized mixed FEMs for nonlinear parabolic equations. We point out that examples shown in this section do not satisfy the assumptions assumed in previous works [6, 7, 8, 16, 17, 23, 28]. We present two typical nonlinear equations with different $f(u, \nabla u)$.

Example 4.1. *The first one is the Allen–Cahn type equation*

$$
\begin{cases}
\dfrac{\partial u}{\partial t} - \Delta u + u^3 - u = 0\,, & in\ \Omega \times (0, T], & (4.1) \\[2mm]
u(\boldsymbol{x}, t) = u^0(\boldsymbol{x})\,, & in\ \Omega, & (4.2) \\[2mm]
u = 0\,, & on\ \partial\Omega, & (4.3)
\end{cases}
$$

Conventional Lagrange FEMs have been widely used to solve the above equation. However, one might consider using a mixed method for the above Allen–Cahn equations in the hope of getting a better approximation of the flux ∇u, which is needed in the case of coupling ∇u with Navier–Stokes equations, see [13, 21].

Example 4.2. *The second one is the viscous Burgers' equation*

$$
\begin{cases}
\dfrac{\partial u}{\partial t} - \Delta u + (\mathbf{b} \cdot \nabla u)u = 0\,, & in\ \Omega \times (0, T], & (4.4) \\[2mm]
u(\boldsymbol{x}, t) = u^0(\boldsymbol{x})\,, & in\ \Omega, & (4.5) \\[2mm]
u = 0\,, & on\ \partial\Omega. & (4.6)
\end{cases}
$$

where $\mathbf{b} = [1, 1, 1]^T$.

Here we combines the nonlinear terms in the last two examples and study the following artificial problem

$$
\begin{cases}
\dfrac{\partial u}{\partial t} - \Delta u + (\mathbf{b} \cdot \nabla u)\,u + u^3 - u = 0\,, & in\ \Omega \times (0, T], & (4.7) \\[2mm]
u(\boldsymbol{x}, t) = u^0(\boldsymbol{x})\,, & in\ \Omega, & (4.8) \\[2mm]
u = 0\,, & on\ \partial\Omega. & (4.9)
\end{cases}
$$

A linearized mixed FEMs is to look for $(\boldsymbol{\sigma}_h^n, u_h^n) \in \mathbf{H}_h^r(\Omega) \times V_h^r(\Omega)$ such that for $n = 1, 2, \ldots,$

$$
\begin{cases}
(\boldsymbol{\sigma}_h^n, \boldsymbol{\chi}_h) + (u_h^n, \mathrm{div}\boldsymbol{\chi}_h) = 0\,, & \forall \boldsymbol{\chi}_h \in \mathbf{H}_h^r(\Omega)\,, & (4.10) \\[2mm]
(D_\tau u_h^n, v_h) - (\mathrm{div}\boldsymbol{\sigma}_h^n, v_h) + (\mathbf{b} \cdot \boldsymbol{\sigma}_h^{n-1} u_h^{n-1}, v_h) & \\[1mm]
\qquad\qquad + ((u_h^{n-1})^3 - u_h^{n-1}, v_h) = 0\,, & \forall v_h \in V_h^r(\Omega). & (4.11)
\end{cases}
$$

At the initial step, we take $\boldsymbol{\sigma}_h^0 = \Pi_h \nabla u^0(\boldsymbol{x})$ and $u_h^0 = \Pi_h u^0(\boldsymbol{x})$, where Π_h can be the projection defined in (4.14)-(4.15).

For error analysis, we assume that the initial-boundary value problem (4.7)-(4.9) has a unique solution satisfying the regularity condition

$$
u \in L^\infty(0, T; H^{r+2})\,, u_t \in L^\infty(0, T; H^{r+2})\,, u_{tt} \in L^\infty(0, T; L^2). \tag{4.12}
$$

We shall remark that the above regularity assumption might be weakened. In this paper, we emphasize on the unconditional optimal error estimates of the linearized mixed FEMs (4.10)-(4.11). We state our main results on error analysis in the following theorem. The proof will be given in the next subsection 4.2.

Theorem 4.1. *Under the regularity assumption , there exist two positive constants h_0 and τ_0 such that when $h < h_0$ and $\tau < \tau_0$, the mixed FEM systems (4.10)-(4.11) are uniquely solvable and the following error estimates hold*

$$\max_{0 \le n \le N} \left(\|u_h^n - u^n\|_{L^2}^2 + \tau \sum_{m=1}^n \|\boldsymbol{\sigma}_h^m - \boldsymbol{\sigma}^m\|_{L^2}^2 \right) \le C_* (\tau^2 + h^{2r+2}), \tag{4.13}$$

where C_* is a positive constant independent of n, h and τ.

To prove the above theorem, we need to define a projector $\Pi_h : (\mathbf{H}(\mathrm{div}; \Omega), L^2(\Omega)) \to (\mathbf{H}_h^r(\Omega), V_h^r(\Omega))$. Given the exact solution $(\boldsymbol{\sigma}, u)$ to (4.7)-(4.9) at any time $t \in (0, T]$, we seek $(\Pi_h \boldsymbol{\sigma}, \Pi_h u) \in (\mathbf{H}_h^r(\Omega), V_h^r(\Omega))$ such that

$$\begin{cases} (\Pi_h \boldsymbol{\sigma}_h, \boldsymbol{\chi}_h) + (\Pi_h u_h, \mathrm{div} \boldsymbol{\chi}_h) = 0, & \forall \boldsymbol{\chi}_h \in \mathbf{H}_h^r(\Omega), & (4.14) \\ (\mathrm{div}\, \Pi_h \boldsymbol{\sigma}_h, v_h) = (\mathrm{div}\, \boldsymbol{\sigma}, v_h), & \forall v_h \in V_h^r(\Omega). & (4.15) \end{cases}$$

We denote the projection error functions by

$$\theta_{\boldsymbol{\sigma}} = \Pi_h \boldsymbol{\sigma} - \boldsymbol{\sigma}, \quad \theta_u = \Pi_h u - u, \tag{4.16}$$

From the classical error estimates for mixed methods [3, 12, 27], we have

$$\|\theta_u\|_{L^2} + \|\theta_{\boldsymbol{\sigma}}\|_{L^2} \le C h^{r+1} \|u\|_{H^{r+1}}, \quad \left\| \frac{\partial \theta_u}{\partial t} \right\|_{L^2} \le C h^{r+1} \left\| \frac{\partial u}{\partial t} \right\|_{H^{r+1}}. \tag{4.17}$$

Moreover, the following uniform boundedness estimates can be proved by using an inverse inequality

$$\|\Pi_h \boldsymbol{\sigma}\|_{L^p} + \|\Pi_h u\|_{L^p} \le C, \quad \text{for } 1 \le p \le 6. \tag{4.18}$$

With the above projection error estimates, we only need to analyze the error functions

$$e_{\boldsymbol{\sigma}}^n = \boldsymbol{\sigma}_h^n - \Pi_h \boldsymbol{\sigma}^n, \quad e_u^n = u_h^n - \Pi_h u^n, \quad \text{for } n = 1, 2, \ldots, N. \tag{4.19}$$

We provide an unconditionally optimal estimates for $\{(e_{\boldsymbol{\sigma}}^n, e_u^n)\}_{n=0}^N$ in the next subsection.

4.2 Proof of Theorem 4.1

Proof: The existence and uniqueness of numerical solutions to the linearized mixed FEMs (4.10)-(4.11) follow directly from that at each time step, the coefficient matrix is invertable. Here we prove the following inequality for $n = 0, \ldots, N$

$$\|e_u^n\|_{L^2}^2 + \sum_{m=1}^n \tau \|e_{\boldsymbol{\sigma}}^m\|_{L^2}^2 \le \frac{C_*}{2} (\tau^2 + h^{2r+2}), \tag{4.20}$$

by mathematical induction. Since

$$\|e_u^0\|_{L^2}^2 + \|e_{\boldsymbol{\sigma}}^0\|_{L^2}^2 = 0,$$

(4.20) holds for $n = 0$. We can assume that (4.20) holds for $n \le k - 1$ for some $k \ge 1$. We shall find a constant C_*, which is independent of n, h, τ, such that (4.20) holds for $n \le k$.

At time step t_n, by noting the projection (4.14)-(4.15), the exact solution $(\boldsymbol{\sigma}, u)$ satisfies

$$(\Pi_h \boldsymbol{\sigma}^n, \boldsymbol{\chi}_h) + (\Pi_h u^n, \operatorname{div}\boldsymbol{\chi}_h) = 0, \qquad\qquad \forall \boldsymbol{\chi}_h \in \mathbf{H}_h^r(\Omega), \qquad (4.21)$$

$$(D_\tau u^n, v_h) - (\operatorname{div}\Pi_h \boldsymbol{\sigma}^n, v_h) = -(\mathbf{b} \cdot \boldsymbol{\sigma}^{n-1} u^{n-1}, v_h)$$
$$- ((u^{n-1})^3 - u^{n-1}, v_h) - (R_u^n, v_h), \qquad \forall v_h \in V_h^r(\Omega), \qquad (4.22)$$

where

$$R_u^n = D_\tau u^n - \frac{\partial u}{\partial t}\Big|_{t_n} + (\mathbf{b} \cdot \nabla u^n u^n - \mathbf{b} \cdot \nabla u^{n-1} u^{n-1}) + ((u^{n-1})^3 - u^{n-1}) - ((u^n)^3 - u^n)$$

stands for the truncation error. Subtracting (4.21)-(4.22) from (4.10)-(4.11), respectively, we obtain the error equations

$$(e_{\boldsymbol{\sigma}}^n, \boldsymbol{\chi}_h) + (e_u^n, \operatorname{div}\boldsymbol{\chi}_h) = 0, \qquad\qquad \forall \boldsymbol{\chi}_h \in \mathbf{H}_h^r(\Omega), \quad (4.23)$$

$$(D_\tau e_u^n, v_h) - (\operatorname{div}e_{\boldsymbol{\sigma}}^n, v_h) = (\mathbf{b} \cdot \nabla u^{n-1} u^{n-1} - \mathbf{b} \cdot \boldsymbol{\sigma}_h^{n-1} u_h^{n-1}, v_h)$$
$$- (((u^{n-1})^3 - u^{n-1}) - ((u_h^{n-1})^3 - u_h^{n-1}), v_h) - (D_\tau \theta_u^n - R_u^n, v_h), \quad \forall v_h \in V_h^r(\Omega). \quad (4.24)$$

Taking $(\boldsymbol{\chi}_h, v_h) = (e_{\boldsymbol{\sigma}}^n, e_u^n)$ into the above error equations (4.23)-(4.24) and summing up the results lead to

$$(D_\tau e_u^n, e_u^n) + \|e_{\boldsymbol{\sigma}}^n\|_{L^2}^2$$
$$= (\mathbf{b} \cdot \nabla u^{n-1} u^{n-1} - \mathbf{b} \cdot \boldsymbol{\sigma}_h^{n-1} u_h^{n-1}, e_u^n)$$
$$+ (((u^{n-1})^3 - u^{n-1}) - ((u_h^{n-1})^3 - u_h^{n-1}), e_u^n) - (D_\tau \theta_u^n - R_u^n, e_u^n) \qquad (4.25)$$

We estimate the right hand side of (4.25) term by term. By the regularity assumption on the exact solution u in (4.12) and the projection error (4.17), the last term in the right hand side of (4.25) can be bounded by

$$(D_\tau \theta_u^n - R_u^n, e_u^n) \leq C\|e_u^n\|_{L^2}^2 + C\tau^2 + Ch^{2r+2} \qquad (4.26)$$

By noting that the assumption (4.20) holds for $n \leq k-1$, we can derive that if $\tau \leq h^{r+1}$

$$\|e_u^n\|_{L^3} \leq h^{-\frac{1}{2}}\|e_u^n\|_{L^2} \leq h^{-\frac{1}{2}}\sqrt{\frac{C_*}{2}(\tau^2 + h^{2r+2})} \leq \sqrt{C_*}h^{r+\frac{1}{2}}, \qquad (4.27)$$

where an inverse inequality is used. If $h^{r+1} \leq \tau$, by using the discrete Sobolev embedding inequality in Theorem 3.2, we have

$$\|e_u^n\|_{L^3} \leq C\|e_{\boldsymbol{\sigma}}^n\|_{L^2} \leq C\tau^{-\frac{1}{2}}\sqrt{\tau\|e_{\boldsymbol{\sigma}}^n\|_{L^2}^2} \leq C\tau^{-\frac{1}{2}}\sqrt{\frac{C_*}{2}(\tau^2 + h^{2r+2})} \leq C\sqrt{C_*}\tau^{\frac{1}{2}}. \qquad (4.28)$$

Therefore, for any given ϵ, we have in both cases

$$\|e_u^n\|_{L^3} \leq \max\left\{\sqrt{C_*}h^{r+\frac{1}{2}}, C\sqrt{C_*}\tau^{\frac{1}{2}}\right\} \leq \epsilon, \quad \text{for } n = 1, \ldots, k-1 \qquad (4.29)$$

if we require that $\tau \leq \tau_0$ and $h \leq h_0$, where τ_0 and h are two small constant numbers. Now we estimate the two nonlinear terms in the right hand side of (4.25). The first nonlinear term can

10

be bounded by

$$
(\mathbf{b} \cdot \nabla u^{n-1} u^{n-1} - \mathbf{b} \cdot \boldsymbol{\sigma}_h^{n-1} u_h^{n-1}, e_u^n)
$$
$$
= -(\mathbf{b} \cdot \nabla u^{n-1}(\theta_u^{n-1} + e_u^{n-1}), e_u^n) - (\mathbf{b} \cdot (\theta_{\boldsymbol{\sigma}}^{n-1} + e_{\boldsymbol{\sigma}}^{n-1})\Pi_h u^{n-1}, e_u^n)
$$
$$
- (\mathbf{b} \cdot (\theta_{\boldsymbol{\sigma}}^{n-1} + e_{\boldsymbol{\sigma}}^{n-1}) e_u^{n-1}, e_u^n)
$$
$$
\leq \|\mathbf{b} \cdot \nabla u^{n-1}\|_{L^\infty} \|\theta_u^{n-1} + e_u^{n-1}\|_{L^2} \|e_u^n\|_{L^2} + \|\mathbf{b} \cdot (\theta_{\boldsymbol{\sigma}}^{n-1} + e_{\boldsymbol{\sigma}}^{n-1})\|_{L^2} \|\Pi_h u^{n-1}\|_{L^6} \|e_u^n\|_{L^3}
$$
$$
+ \|\mathbf{b} \cdot (\theta_{\boldsymbol{\sigma}}^{n-1} + e_{\boldsymbol{\sigma}}^{n-1})\|_{L^2} \|e_u^{n-1}\|_{L^3} \|e_u^n\|_{L^6}
$$
$$
\leq C\|e_u^{n-1}\|_{L^2}^2 + C\|e_u^n\|_{L^2}^2 + Ch^{2r+2} + C(\|e_{\boldsymbol{\sigma}}^{n-1}\|_{L^2} + h^{r+1})\|e_u^n\|_{L^2}^{\frac{1}{2}} \|e_u^n\|_{L^6}^{\frac{1}{2}}
$$
$$
+ C(\|e_{\boldsymbol{\sigma}}^{n-1}\|_{L^2} + h^{r+1})\|e_u^{n-1}\|_{L^3} \|e_u^n\|_{L^6}
$$
$$
\leq C(\|e_{\boldsymbol{\sigma}}^{n-1}\|_{L^2} + h^{r+1})\|e_u^n\|_{L^2}^{\frac{1}{2}} \|e_{\boldsymbol{\sigma}}^n\|_{L^2}^{\frac{1}{2}} + C(\|e_{\boldsymbol{\sigma}}^{n-1}\|_{L^2} + h^{r+1})\|e_u^{n-1}\|_{L^3} \|e_{\boldsymbol{\sigma}}^n\|_{L^2}
$$
$$
+ C\|e_u^{n-1}\|_{L^2}^2 + C\|e_u^n\|_{L^2}^2 + Ch^{2r+2} \tag{4.30}
$$

By using Young's inequality, we have

$$
C(\|e_{\boldsymbol{\sigma}}^{n-1}\|_{L^2} + h^{r+1})\|e_u^n\|_{L^2}^{\frac{1}{2}} \|e_{\boldsymbol{\sigma}}^n\|_{L^2}^{\frac{1}{2}} \leq \epsilon(\|e_{\boldsymbol{\sigma}}^{n-1}\|_{L^2}^2 + \|e_{\boldsymbol{\sigma}}^n\|_{L^2}^2) + \epsilon^{-1} C\|e_u^n\|_{L^2}^2 + \epsilon^{-1} Ch^{2r+2}. \tag{4.31}
$$

And by using the (4.29), we can derive

$$
C(\|e_{\boldsymbol{\sigma}}^{n-1}\|_{L^2} + h^{r+1})\|e_u^{n-1}\|_{L^3} \|e_{\boldsymbol{\sigma}}^n\|_{L^2} \leq \epsilon(\|e_{\boldsymbol{\sigma}}^{n-1}\|_{L^2}^2 + \|e_{\boldsymbol{\sigma}}^n\|_{L^2}^2) + \epsilon^{-1} Ch^{2r+2} \tag{4.32}
$$

where we shall require τ and h are smaller than certain constants. Substituting the last two inequality into (4.30) gives

$$
(\mathbf{b} \cdot \nabla u^{n-1} u^{n-1} - \mathbf{b} \cdot \boldsymbol{\sigma}_h^{n-1} u_h^{n-1}, e_u^n)
$$
$$
\leq \epsilon(\|e_{\boldsymbol{\sigma}}^{n-1}\|_{L^2}^2 + \|e_{\boldsymbol{\sigma}}^n\|_{L^2}^2) + \epsilon^{-1} C\|e_u^n\|_{L^2}^2 + \epsilon^{-1} Ch^{2r+2} \tag{4.33}
$$

Next, the second nonlinear term in the right hand side of (4.25) can be bounded by

$$
(((u^{n-1})^3 - u^{n-1}) - ((u_h^{n-1})^3 - u_h^{n-1}), e_u^n)
$$
$$
\leq ((u^{n-1})^3 - (u_h^{n-1})^3, e_u^n) + C\|e_u^{n-1}\|_{L^2}^2 + C\|e_u^n\|_{L^2}^2 + Ch^{2r+2}
$$
$$
\leq (-3(u^{n-1})^2(\theta_u^{n-1} + e_u^{n-1}) + 3u^{n-1}(\theta_u^{n-1} + e_u^{n-1})^2 - (\theta_u^{n-1} + e_u^{n-1})^3, e_u^n)
$$
$$
+ C\|e_u^{n-1}\|_{L^2}^2 + C\|e_u^n\|_{L^2}^2 + Ch^{2r+2}
$$
$$
\leq C|((e_u^{n-1})^3, e_u^n)| + C|(\theta_u^{n-1}(e_u^{n-1})^2, e_u^n)| + C\|e_u^{n-1}\|_{L^2}^2 + C\|e_u^n\|_{L^2}^2 + Ch^{2r+2}
$$
$$
\leq C\|e_u^{n-1}\|_{L^3} \|e_u^{n-1}\|_{L^3} \|e_u^{n-1}\|_{L^6} \|e_u^n\|_{L^6} + C\|\theta_u^{n-1}\|_{L^3} \|e_u^{n-1}\|_{L^3} \|e_u^{n-1}\|_{L^6} \|e_u^n\|_{L^6}
$$
$$
+ C\|e_u^{n-1}\|_{L^2}^2 + C\|e_u^n\|_{L^2}^2 + Ch^{2r+2}
$$
$$
\leq C\epsilon^2 \|e_{\boldsymbol{\sigma}}^{n-1}\|_{L^2} \|e_{\boldsymbol{\sigma}}^n\|_{L^2} + C\epsilon\|e_{\boldsymbol{\sigma}}^{n-1}\|_{L^2} \|e_{\boldsymbol{\sigma}}^n\|_{L^2} + C\|e_u^{n-1}\|_{L^2}^2 + C\|e_u^n\|_{L^2}^2 + Ch^{2r+2}
$$
$$
\leq \epsilon(\|e_{\boldsymbol{\sigma}}^{n-1}\|_{L^2}^2 + \|e_{\boldsymbol{\sigma}}^n\|_{L^2}^2) + C\|e_u^{n-1}\|_{L^2}^2 + C\|e_u^n\|_{L^2}^2 + Ch^{2r+2} \tag{4.34}
$$

where we have used (4.29) with requirement τ and h are smaller than certain constants and the embedding equality in Theorem 3.2.

Finally, substituting estimates (4.26), (4.33) and (4.34) into (4.25), we obtain

$$
(D_\tau e_u^n, e_u^n) + \|e_{\boldsymbol{\sigma}}^n\|_{L^2}^2
$$
$$
\leq \epsilon\|e_{\boldsymbol{\sigma}}^{n-1}\|_{L^2}^2 + \epsilon^{-1} C\|e_u^{n-1}\|_{L^2}^2 + \epsilon^{-1} C\|e_u^n\|_{L^2}^2 + \epsilon^{-1} C(\tau^2 + h^{2r+2}), \tag{4.35}
$$

Then, we chose a small ϵ and summing up the last inequality for the index $n = 1, 2, \ldots, k$ to deduce that

$$
\|e_u^n\|_{L^2}^2 + \tau \sum_{m=1}^n \|e_{\boldsymbol{\sigma}}^m\|_{L^2}^2 \leq \tau C \sum_{m=1}^n \|e_u^m\|_{L^2}^2 + \tau C \sum_{m=1}^n (\tau^2 + h^{2r+2}), \tag{4.36}
$$

Thanks to the discrete Gronwall's inequality in Lemma 2.2, when $C\tau \leq \frac{1}{2}$, we have

$$
\|e_u^n\|_{L^2}^2 + \|e_\sigma^n\|_{L^2}^2 + \tau \sum_{m=1}^{n} \left(\|e_\sigma^m\|_{L^2}^2 + \|\mathrm{div}e_\sigma^m\|_{L^2}^2 \right)
$$
$$
\leq C \exp\left(\frac{TC}{1 - C\tau} \right) (\tau^2 + h^{2r+2})
$$
$$
\leq C \exp(2TC)(\tau^2 + h^{2r+2}) \tag{4.37}
$$

Thus, (4.20) holds for $n = k$ if we take $\frac{C_*}{2} \geq C \exp(2TC)$. We complete the induction.

Theorem 4.1 follows immediately from the the projection error estimates and the above inequality. □

5   Numerical examples

In this section, we provide numerical experiments in both two and three dimensional spaces to confirm our theoretical results in Theorem 4.1 and show the efficiency of the linearized mixed FEMs. The computations are carried out with the free software FEniCS [24].

Example 5.1. First we consider an artificial problem in two dimensional space

$$
\begin{cases}
\dfrac{\partial u}{\partial t} - \Delta u + u^3 = g\,, & \text{in } \Omega & (5.1) \\[2mm]
u = 0, & \text{on } \partial\Omega & (5.2) \\[2mm]
u = u_0(x), & \text{in } \Omega, & (5.3)
\end{cases}
$$

where we take $\Omega = (0,1) \times (0,1)$. The function g is chosen correspondingly to the exact solution

$$
u(t,x,y) = \exp(t)xy(1-x)(1-y).
$$

We set the terminal time $T = 1.0$ in this example. This example had been tested in [23], where a nonlinear backward Euler mixed FEM with a two-grid algorithm was used.
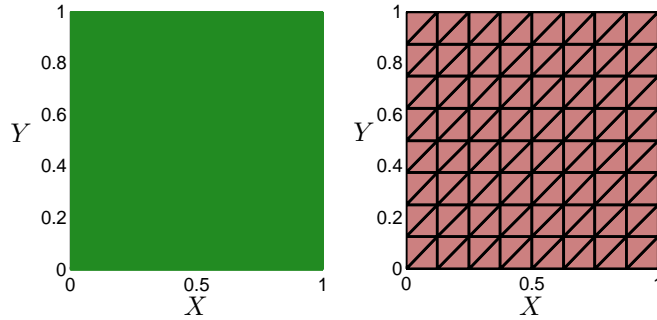

Figure 1: A uniform triangular mesh on the unit square with $M = 8$.

We use a uniform triangular mesh with $M + 1$ vertices in each direction, where $h = \frac{\sqrt{2}}{M}$ (see Figure 1 for illustration with $M = 8$). We solve (5.1)-(5.3) by the proposed linearized mixed FEMs (4.10)-(4.11) with $r = 0, 1, 2$, respectively. To demonstrate the $O(\tau + h^r)$ convergence of L^2-norm errors of u_h and σ_h, we set $\tau = \left(\frac{1}{M}\right)^{r+1}$ in our computation. The L^2-norm errors of the scheme are shown in Table 1. From Table 1, we can see that the L^2-norm errors for u_h and σ_h are proportional to h^{r+1}, which confirms the optimal convergence rates clearly.

12

Table 1: L^2-norm errors of u_h and $\boldsymbol{\sigma}_h$ on the unit square (Example 5.1).

$\mathbf{H}_h^0 \times V_h^0 \quad \tau = \frac{1}{M}$	$\|u^N - u_h^N\|_{L^2}$	$\|\boldsymbol{\sigma}^N - \boldsymbol{\sigma}_h^N\|_{L^2}$
$M = 32$	2.9850e-03	1.2659e-02
$M = 64$	1.4928e-03	6.3329e-03
$M = 128$	7.4643e-04	3.1668e-03
Order	9.9983e-01	9.9951e-01
$\mathbf{H}_h^1 \times V_h^1 \quad \tau = \frac{1}{M^2}$	$\|u^N - u_h^N\|_{L^2}$	$\|\boldsymbol{\sigma}^N - \boldsymbol{\sigma}_h^N\|_{L^2}$
$M = 16$	2.3732e-04	1.0243e-03
$M = 32$	5.9385e-05	2.5731e-04
$M = 64$	1.4850e-05	6.4475e-05
Order	1.9992e+00	1.9949e+00
$\mathbf{H}_h^2 \times V_h^2 \quad \tau = \frac{1}{M^3}$	$\|u^N - u_h^N\|_{L^2}$	$\|\boldsymbol{\sigma}^N - \boldsymbol{\sigma}_h^N\|_{L^2}$
$M = 8$	4.2973e-05	1.4866e-04
$M = 16$	5.3949e-06	1.8728e-05
$M = 32$	6.7509e-07	2.3501e-06
Order	2.9961e+00	2.9916e+00

To test the stability of the proposed method, we solve (5.1)-(5.3) by the linearized mixed FEMs (4.10)-(4.10) with three fixed time steps $\tau = 0.1$, 0.05, 0.01 on gradually refined meshes with $M = 8$, 16, 32, 64 and 128, where we take $r = 1$, i.e., $\mathbf{H}_h^1(\Omega) \times V_h^1(\Omega)$ is used. We plot in Figure 2 the L^2 errors of u_h and $\boldsymbol{\sigma}_h$. From Figure 2, we can see that for each fixed τ, when the mesh is refined gradually, each L^2 error converges to a small constant of $O(\tau)$. This shows that the proposed linearized mixed FEM is unconditionally stable, i.e., the method does not require mesh ratio restriction $\tau \leq Ch^\alpha$ for a certain $\alpha > 0$.
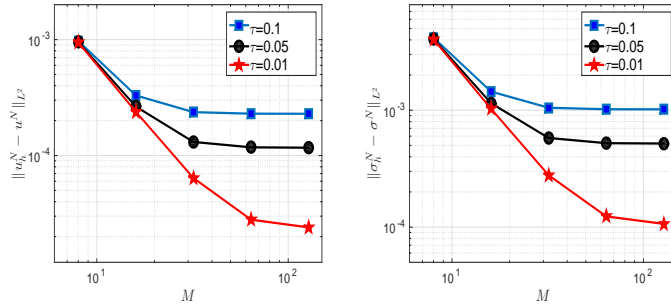

Figure 2: L^2 errors of u_h and $\boldsymbol{\sigma}_h$ with $\mathbf{H}_h^1 \times V_h^1$ on gradually refined meshes with fixed τ (Example 5.1).

Example 5.2. In this example we test the performance of the linearized mixed FEMs for the

following three-dimensional problem

$$
\begin{cases}
\dfrac{\partial u}{\partial t} - \Delta u + (\mathbf{b} \cdot \nabla u)u + u^3 - u = g\,, & \text{in } \Omega & (5.4) \\[2mm]
u = 0, & \text{on } \partial\Omega & (5.5) \\[2mm]
u = u_0(x), & \text{in } \Omega, & (5.6)
\end{cases}
$$

where we take the unit cube $\Omega = (0,1) \times (0,1) \times (0,1)$. The function g is chosen correspondingly to the exact solution

$$u(t,x,y) = \exp(-t)\sin(\pi x)\sin(2\pi y)z(1-z).$$

A uniform tetrahedral mesh with $M+1$ vertices in each direction are used, where $h = \frac{\sqrt{3}}{M}$. We solve the above equation (5.4)-(5.6) by the proposed linearized mixed FEMs (4.10)-(4.11) with $(\mathbf{H}_h^r(\Omega) \times V_h^r(\Omega))$ for $r = 0, 1$, respectively. We also set $\tau = \left(\frac{1}{M}\right)^{r+1}$ and terminal time $T = 1.0$ in our computations. We present the L^2-norm errors of the scheme in Table 2. Again, we can see clearly that the L^2-norm errors of u_h and $\boldsymbol{\sigma}_h$ are proportional to h^{r+1}, for $r = 0, 1$, respectively. This indicates that the convergence rate of the linearized mixed FEM (4.10)-(4.11) is optimal in three-dimensional space.

Table 2: L^2-norm errors of u_h and $\boldsymbol{\sigma}_h$ on the unit cube (Example 5.2).

$\mathbf{H}_h^0 \times V_h^0 \quad \tau = \frac{1}{M}$	$\|u^N - u_h^N\|_{L^2}$	$\|\boldsymbol{\sigma}^N - \boldsymbol{\sigma}_h^N\|_{L^2}$
$M = 10$	5.1823e-03	4.2003e-02
$M = 20$	2.6285e-03	2.1121e-02
$M = 40$	1.3189e-03	1.0575e-02
Order	9.8711e-01	9.9490e-01
$\mathbf{H}_h^1 \times V_h^1 \quad \tau = \frac{1}{M^2}$	$\|u^N - u_h^N\|_{L^2}$	$\|\boldsymbol{\sigma}^N - \boldsymbol{\sigma}_h^N\|_{L^2}$
$M = 8$	8.0631e-04	5.4993e-03
$M = 16$	2.0467e-04	1.3935e-03
$M = 32$	5.1364e-05	3.4997e-04
Order	1.9862e+00	1.9870e+00

To test the stability of the proposed method, we solve (5.4)-(5.6) by the linearized mixed FEMs (4.10)-(4.10) with three fixed time steps $\tau = 0.1, 0.05, 0.01$ on gradually refined meshes with $M = 10, 20, 30, 40$ and 50, where $\mathbf{H}_h^1(\Omega) \times V_h^1(\Omega)$ is used for spatial discretization. We plot in Figure 3 the L^2 errors of u_h and $\boldsymbol{\sigma}_h$. From Figure 3, we can see that the size of the time step τ affects the accuracy but not the stability of the scheme. This shows that the proposed linearized mixed FEMs are unconditionally stable in three-dimensional space.

6   Conclusion

We have proved a discrete Sobolev embedding inequality for the Raviart–Thomas mixed FEMs for second order elliptic equations. The essential idea is to control the L^p norm of u_h by the discrete Sobolev norm $\|u_h\|_{DG}$ and then prove that $\|u_h\|_{DG}$ is bounded by $\|\boldsymbol{\sigma}_h\|_{L^2}$. In this paper we focus on the Raviart–Thomas mixed FEMs. However, it is easy to see that the results can be extended to other stable elements, such as Brezzi–Douglas–Marini(BDM) mixed FEMs.
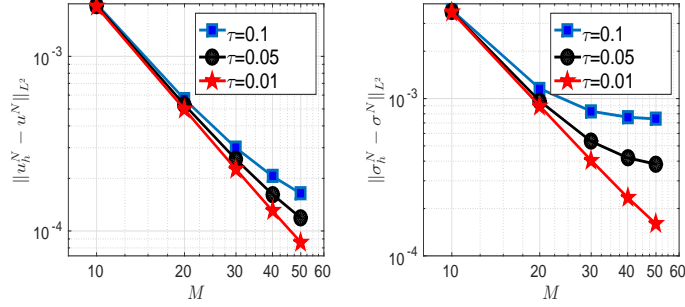
Figure 3: L^2 errors of u_h and $\boldsymbol{\sigma}_h$ with $\mathbf{H}_h^1 \times V_h^1$ on gradually refined meshes with fixed τ (Example 5.2).

We shall remark that in our proof there is no requirement on the domain Ω. In this paper, we only consider homogeneous Dirichlet boundary conditions. It should be noted that extension to other boundary conditions can also be obtained with slightly change of notations. By using the proved discrete Sobolev inequality, we have established an unconditionally optimal error estimates for mixed FEMs of nonlinear parabolic equations. We point out that the discrete Sobolev embedding inequalities proved in this work can be used to analyze mixed FEMs of more general nonlinear parabolic systems.

Acknowledgments

References

[1] T. Arbogast, D. Estep, B. Sheehan and S. Tavener, A posteriori error estimates for mixed finite element and finite volume methods for parabolic problems coupled through a boundary, *SIAM/ASA J. Uncertain. Quantif.*, 3(2015), pp. 169–198.

[2] T. Arbogast and M. Wheeler, A characteristics-mixed finite element method for advection-dominated transport problems, *SIAM J. Numer. Anal.*, 32(1995), pp. 404–424.

[3] D. Boffi, F. Brezzi and M. Fortin, *Mixed Finite Element Methods and Applications*, Springer, Heidelberg, 2013.

[4] F. Brezzi, L. Marini, S. Micheletti, P. Pietra, R. Sacco, and S. Wang, Discretization of Semiconductor Device Problems (I), *Handbook of Numerical Analysis XIII*, special Volume on Numerical Methods in Electromagnetics, North-Holland, Amsterdam, 2005, pp. 317–442.

[5] A. Buffa and C. Ortner, Compact embeddings of broken Sobolev spaces and applications, *IMA J. Numer. Anal.*, 29(2009), pp. 827–855.

[6] L. Chen and Y. Chen, Two-grid method for nonlinear reaction-diffusion equations by mixed finite element methods, *J. Sci. Comput.*, 49(2011), pp. 383–401.

[7] Y. Chen, H. Liu and S. Liu, Analysis of two-grid methods for reaction-diffusion equations by expanded mixed finite element methods, *Int. J. Numer. Meth. Engng.*, 69(2007), pp. 408–422.

[8] Y. Chen, Y. Huang and D. Yu, A two-grid method for expanded mixed finite-element solution of semilinear reaction-diffusion equations, *Int. J. Numer. Meth. Eng.*, 57(2003), pp. 193–209.

[9] D. Di Pietro and A. Ern, Discrete functional analysis tools for discontinuous Galerkin methods with application to the incompressible Navier–Stokes equations, *Math. Comp.*, 79(2010), pp. 1303–1330.

[10] C. Dawson, S. Sun and M. Wheeler, Compatible algorithm for coupled flow and transport, *Comput. Methods Appl. Mech. Engrg.*, 193(2004), pp. 2562–2580

[11] H. Egger and J. Schoberl, A hybrid mixed discontinuous Galerkin finite-element method for convection-diffusion problems, *IMA J. Numer. Anal.*, 30 (2010), pp. 1206–1234.

[12] A. Ern and J. Guermond, *Theory and Practice of Finite Elements*, Applied Mathematical Sciences, 159, Springer–Verlag, New York, 2004.

[13] X. Feng, Y. He and C. Liu, Analysis of finite element approximations of a phase field model for two phase fluids, *Math. Comp.*, 76(2007), pp. 539–571.

[14] S. Gadau and A. Jungel, A three-dimensional mixed finite-element approximation of the semiconductor energy-transport equations, *SIAM J. Sci. Comput.*, 31(2008/09), pp. 1120–1140.

[15] H. Gao, B. Li and W. Sun, Optimal error estimates of linearized Crank–Nicolson Galerkin FEMs for the time-dependent Ginzburg–Landau equations in superconductivity, *SIAM J. Numer. Anal.*, 52(2014), pp. 1183–1202.

[16] M. Garcia, Improved error estimates for mixed finite element approximations for nonlinear parabolic equations: the continuously-time case, *Numer. Methods Partial Different. Equations*, 10(1994), pp. 129–149.

[17] M. Garcia, Improved error estimates for mixed finite element approximations for nonlinear parabolic equations: the discrete-time case, *Numer. Methods Partial Different. Equations*, 10(1994), pp. 149–169.

[18] J. Heywood and R. Rannacher, Finite element approximation of the nonstationary Navier–Stokes problem IV: Error analysis for second-order time discretization, *SIAM J. Numer. Anal.*, 27(1990), pp. 353–384.

[19] S. Holst, A. Jungel and P. Pietra, An adaptive mixed scheme for energy-transport simulations of field-effect transistors. *SIAM J. Sci. Comput.* 25(2004), pp. 1698–1716.

[20] Y. Hou, B. Li and W. Sun, Error estimates of splitting Galerkin methods for heat and sweat transport in textile materials, *SIAM J. Numer. Anal.*, 51(2013), pp. 88–111.

[21] J. Hua, P. Lin, C. Liu and Q. Wang, Energy law preserving C^0 finite element schemes for phase field models in two-phase flow computations, *J. Comput. Phys.*, 230(2011), pp. 7115–7131.

[22] C. Johnson and V. Thomee, Error estimates for some mixed finite element methods for parabolic type problems, *RAIRO Anal. Numer.*, 15(1981), pp. 41–78.

[23] D. Kim, E. Park and B. Seo, Two-scale product approximation for semilinear parabolic problems in mixed methods, *J. Korean Math. Soc.*, 51(2014), pp. 267–288.

[24] A. Logg, K. Mardal and G. Wells (Eds.), *Automated Solution of Differential Equations by the Finite Element Method*, Springer, Berlin, 2012.

[25] J. Nedelec, Mixed finite elements in $\mathbf{R}^3$, *Numer. Math.*, 35(1980), pp. 315–341.

[26] L. Nirenberg, An extended interpolation inequality, *Ann. Scuola Norm. Sup. Pisa (3)*, 20(1966), pp. 733–737.

[27] P.-A. Raviart and J.-M. Thomas, A mixed finite element method for second order elliptic problems,in Mathematical Aspects of the Finite Element Method, Lecture Notes in Math 606, Springer–Verlag, New York, 1977, pp. 292–315.

[28] L. Wu and M. Allen, A two-grid method for mixed finite-element solution of reaction-diffusion equations. *Numer. Methods Partial Different. Equations*, 15(1999), pp. 317–332.